

# EarthTemp Arctic Sea Surface Temperature Workshop

## Met office, Exeter, 18-19 December 2013

Emmanuelle Autret<sup>(1)</sup>, Steinar Eastwood<sup>(2)</sup>, Owen Embury<sup>(3)</sup>, Emma Fiedler<sup>(4)</sup>, Jacob Høyer<sup>(5)</sup>,  
Ioanna Karagali<sup>(6)</sup>, Pierre Le Borgne<sup>(7)</sup>, Cristina Luis<sup>(2)</sup>, Alison Mc Laren<sup>(4)</sup>, Chris Merchant<sup>(3)</sup>,  
Sonia Péré<sup>(7)</sup>, Jonah Roberts-Jones<sup>(4)</sup>, Hervé Roquet<sup>(7)</sup>

<sup>(1)</sup>Ifremer, <sup>(2)</sup>Met.Norway, <sup>(3)</sup>University of Reading, <sup>(4)</sup>Met.Office, <sup>(5)</sup>Danish Meteorological  
Institute, <sup>(6)</sup>Denmark Technical University, <sup>(7)</sup>Météo-France/CMS,

### 1. Introduction (P. LeBorgne MF/CMS; J. Høyer, DMI)

The Arctic is a strategic area for numerical weather prediction as well as for climate studies due to the recent changes in ice cover, the lack of in situ observations and the Arctic amplification with respect to global warming. These issues were debated during the EarthTemp meeting in Copenhagen for all kind of surfaces, and we now wish to focus on SST. Satellite derived Sea Surface Temperatures (SST) are a major input to operational SST analysis. On the other hand, « Physical » SST retrieval methods using simulated brightness temperatures rely on operational analysis products as guess fields, so mutual interdependency increases. There are indeed specific SST retrieval issues in the Arctic such as: difficult cloud/ice identification, extreme atmospheric conditions, diurnal warming unknowns and the lack of in situ measurements. All these factors impact both satellite SST retrievals and operational analysis.

For the scientists in charge of the corresponding developments, the Arctic is at present the most problematic region of the world ocean. We believe that a joint effort of remote sensing, analysis and Arctic experts could lead to significant progress in that domain.

A workshop has been organized in the framework of the EarthTemp project to give an overview of the problems encountered and to try to organize a joint effort to solve the issues.

The workshop has been organized in 4 sessions over 2 days. The session summary are presented in the text below:

Session 1 (summary by H. Roquet) reviewed the results obtained by operational producers or reprocessing efforts of SST data in the Arctic.

Session 2 (summary by E. Fiedler) presented the results of the European SST analysis covering the Arctic, namely OSTIA, ODYSSEA and the DMI/met.no analysis.

Session 3 (summary by S. Eastwood) addressed the SST variability in the region, essentially induced by diurnal warming

Session 4 (summary by J. Høyer) has been devoted to develop solutions and to organize a joint effort.

The corresponding presentations are available at <https://wiki.met.no/arctic-sst/start>

## 2. Summary report of session 1: SST retrieval in the Arctic (H. Roquet, Meteo-France)

### *2.1 Cloud and Ice detection in the Arctic (Steinar Eastwood, Met Norway)*

Existing cloud/ice detection algorithms are generally not specifically fitted for satellite SST retrieval, and aim at providing an unbiased classification, which can lead to undetected clouds and/or ice. SST retrieval needs a more conservative classification, minimizing the risk of any cloud/ice contamination. This is why an additional cloud/ice masking step is often applied after conventional detection before SST retrieval from satellite infra-red measurements. This step is very important, since sea ice is often less accurately handled by general algorithms, and difficult illumination conditions (twilight) are more frequent at high latitudes.

A probabilistic approach has been developed at Met Norway, based on probability distribution functions (PDFs) in cloud, ice and open water conditions, for some channel combinations sensitive to the presence of clouds and/or ice. For AVHRR and VIIRS, the channel combinations used include for instance  $r0.9/r0.6$  and  $r1.6/r0.6$  ratios. Using the Bayes theorem, the probability of a pixel being cloud, ice and open water can then be inverted from the observations. These PDFs are hence an essential ingredient in the method, and have to be determined using a training data set of satellite observations classified as cloud, ice or open water.

Three different methods can be used to build the classified training data set: manual classification by visual interpretation of the satellite scenes, automatic classification using independent truth data such as SYNOP observations or satellite LIDAR observations (ex : CALIPSO), and automatic classification using an existing cloud mask (ex : PPS, CLAVR-X) applied to the satellite data.

In the case of VIIRS, one year of collocated VIIRS and CALIPSO data have been collected together with sea ice concentration information (needed since CALIPSO data do not allow for water/ice discrimination) in cooperation with SMHI, and corresponding PDFs have been derived for cloud, ice and open water. Similarly, PDFs have also been derived from one year of collocated VIIRS and PPS cloud mask data. A simple test on 11 micron brightness temperatures has been applied to discriminate ice from open water in night conditions, where PPS provides cloud/clear classification only. In this case, different training data sets can lead to significantly different PDFs, for instance for the  $r0.9/r0.6$  ratio.

In the current approach, one-dimensional Gaussian PDFs are adjusted to the empirical histograms obtained from the training data set. Alternatively, one could use PDFs under the form of look-up tables, directly derived from training data, and/or multi-dimensional PDFs. Multi-dimensional PDFs need a large amount of data to be trained.

When a new instrument is coming, new PDFs have to be trained, which can be a time consuming task, and needs a sufficient amount of data from the new instrument to be available.

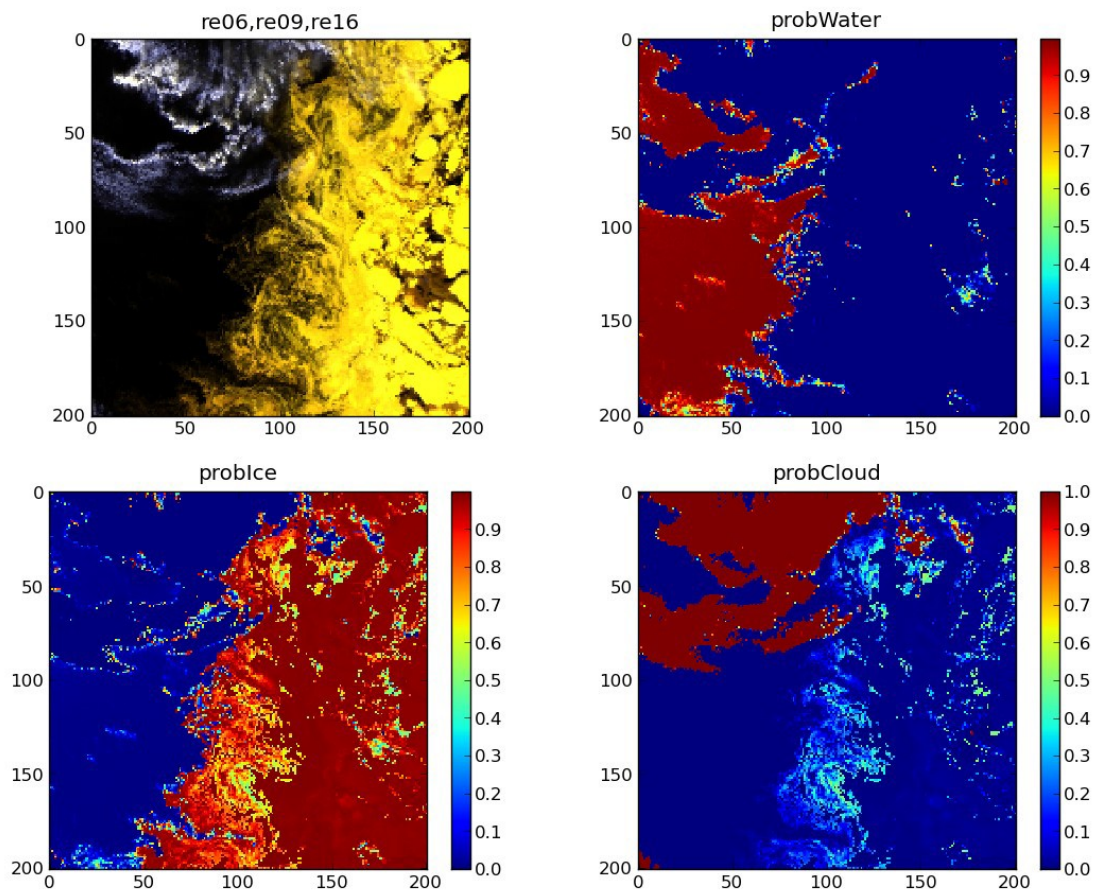


**Fig 1:** Example of open water, ice and cloud probabilities derived AATSR data on 14 April 2009 using the Bayesian classifier developed at Met Norway.

In the case of the Bayesian detection scheme used in the NRT OSI SAF SST processing chain for AVHRR, it had to be adapted quickly to the new VIIRS instrument. This was done by adjusting the existing PDFs for NOAA-19/AVHRR, NOAA-19 and NPP orbits being very close in time. The VIIRS PDFs were derived from a limited data set of collocated VIIRS and AVHRR data, by simply estimating an average shift between VIIRS and AVHRR PDFs. These VIIRS PDFs are now used operationally in the OSI SAF SST processing chain and work fine.

Some of the channel combinations used in the Bayesian detection scheme deviate from the normal day light behaviour when approaching twilight (ex: r0.9/r0.6 ratio, see Fig 2). This effect is parametrized by making the PDFs mean and standard deviation dependent on solar zenith angle for values between 80 and 90 degrees. This dependency found in the observations is also confirmed by visible channel simulations, made with the radiative transfer model libradtran.

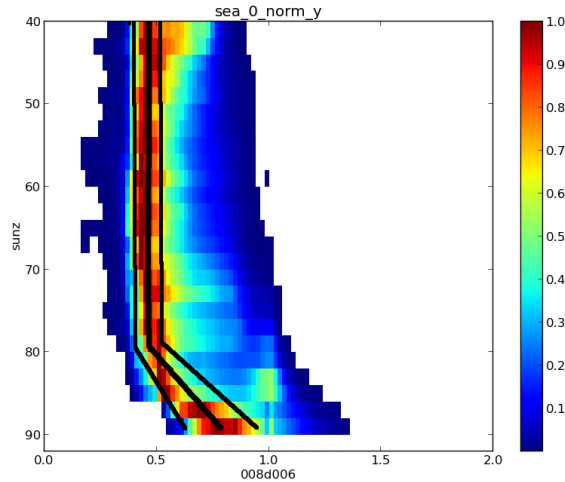


**Fig 2:** Example of AVHRR r0.9/r0.6 probability distribution function (PDF) over open water, as a function of solar zenith angle.

## 2.2 *NRT SST retrieval : multi-spectral algorithm limitations and use of NWP outputs in the Arctic* (Pierre Le Borgne, Météo-France)

SST from METOP-A AVHRR has been produced from summer 2007 up to now at Centre de Météorologie Spatiale (CMS) in the framework of OSI SAF. SST has been produced globally, at full resolution. METOP-A/AVHRR derived SSTs have been validated against drifter measurements on an operational basis. A special attention has been paid to the Arctic, where the SST retrieval conditions are particularly difficult. Previous studies pointed out positive biases by day and negative biases by night in the Arctic. The focus is here on the daytime algorithm (equation 1):

$$\text{SST} = a T_{11} + (b T_{\text{CLI}} + c S_{\theta}) (T_{11} - T_{12}) + d S_{\theta} + e \quad (1)$$

A global simulated Brightness Temperature (BT) data set has been defined at CMS to determine SST algorithms. This data set is based on ECMWF operational forecast profiles. BTs at 3.7, 10.8 and 12.0 microns have been produced by applying RTTOV 10.2 to these profiles.

The operational validation of the OSI SAF SST is based on the Match-up Data Base (MDB). The MDB collects in situ SST measurements from ship, moored or drifting buoys, available through the Global Telecommunication System (GTS) and the coincident full resolution satellite information, within 3 hours from the in situ measurement. The satellite information (calculated SST, brightness temperatures and reflectances) is extracted in a 21x21 pixel box centred on the measurement location providing the coverage of the box by clear pixels is larger than 10%. The MDB includes the in situ measurements (platform ID +SST + auxiliary measures) and all the variables used in METOP SST processing.

The MDB considered here includes 5 year of data. An “Arctic” area has been defined, as North of 60N, for the MDB and for the simulation data set derived from ECMWF profiles. The daytime error statistics are presented in table 1:

	n	$\delta$	$\sigma$
MDB (5 years; QL 3-5)	17405	0.05	0.66
ECMWF simulations data set	534	0.22	0.34

**Table 1:** Daytime validation results of the operational OSI SAF SST algorithm on the 5 year MDB and on the simulation data set derived from ECMWF profiles.

The main trends of the validation errors are given in Fig 3. The validation box cloud coverage has a significant impact on the validation results. For completely clear boxes the bias is positive (0.3K) and becomes negative for clear sky coverage below 60 %. A bias trend with the T10.8 –T12.0 BT difference (DBT in the text below) is also obvious from Fig 2b. The bias increases rapidly for DBT below 1 K. The bias decrease observed for DBT below 0K is due to residual cloudiness. Errors are well reproduced by simulations. Previous detailed analyses of this issue showed that positive biases are related to air temperature inversions, specific to Arctic summer.

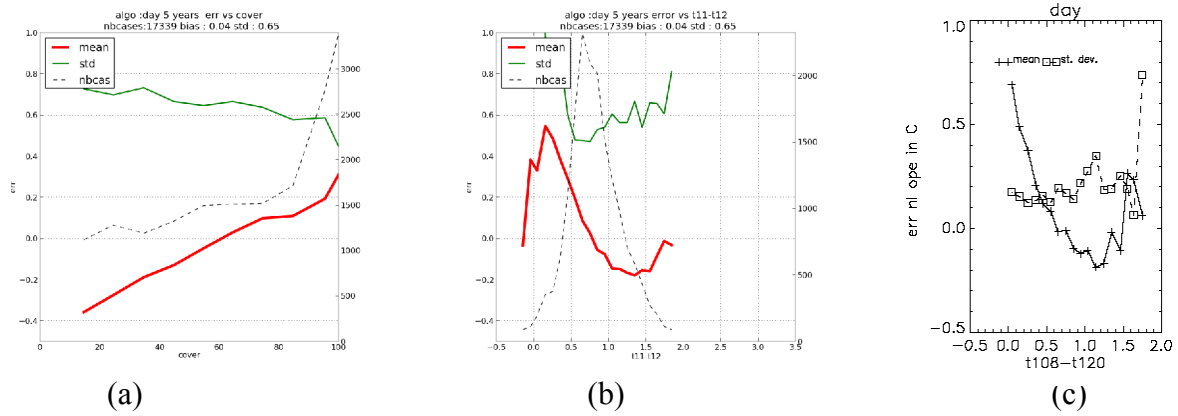


**Fig 3:** a) error versus clear sky coverage on the MDB ; b) error versus DBT on the MDB ; c) error versus DBT on the simulation dataset.

A carefully cloud screened MDB, using quality levels 4 and 5 and clear sky coverage above 80 %, has been built to analyze the algorithm issues. The TS-T10.8 versus DBT relationship is often used to characterize the atmospheric absorption conditions. This relationship is significantly non linear in the Arctic and three distinct absorption regimes can be distinguished (figure not shown). Non linear relationship in the Arctic is not a problem per se and the NLC formalism should be able to offer an adapted solution. We derived optimal NLC (equation 2) regional algorithms on the simulation dataset and on the MDB. We also derived a CASSTA (equation 3) type of algorithm on the MDB only.

$$\text{NLC} \quad \text{SST} = (a + b S_{\theta}) T_{11} + (c + d T_{\text{CLI}} + e S_{\theta}) (T_{11} - T_{12}) + f + g S_{\theta} \quad (2)$$

$$\text{CASSTA} \quad \text{SST} = (a + b S_{\theta}) T_{11} + c + d S_{\theta} \quad (3)$$

6143 cases (cov > 0.8 and QL 4-5)	Operational NLC	Simulation derived regional NLC	Optimal regional NLC	Optimal CASSTA
$\delta$	0.28	0.25	0.	0.
$\sigma$	0.45	0.50	0.44	0.64

**Table 2:** Operational versus Optimal NLC and CASSTA algorithm on the cloud screened 5 year daytime MDB in the Arctic.

The operational versus optimal algorithm results obtained on the cloud screened MDB are presented in table 2. The operational algorithm shows a low standard deviation, close to that of the optimal algorithm, but a positive bias. The simulation derived algorithm shows a positive bias and a rather poor standard deviation. This reveals the limitations of an Arctic sub-sample of a global profile dataset to derive robust algorithms. The CASSTA algorithm is clearly outperformed by any kind of NLC algorithm.

A METOP-A prototype has been built at CMS to test the bias correction method already used operationally at CMS to process the geostationary satellite data. This method uses real time Brightness Temperatures (BTs) derived from applying a fast radiative transfer model (RTTOV) to NWP profiles and using OSTIA as surface temperature. The key step of this method is the BT simulation adjustment. Simulations must indeed be “exact”: they should produce the same BTs as would be observed, given a surface temperature and atmospheric profiles. Due to the limitations of the simulation conditions (RTTOV inaccuracies, NWP atmospheric profile sampling,..) a BT simulation adjustment step is necessary. The only way to derive BT adjustment values is to compare observations and simulations in consistent conditions (when they are actually comparable).

OSTIA is a “foundation” SST and does not resolve the diurnal warming events often encountered in the Arctic. OSTIA based simulations and observations must be compared in diurnal warming free conditions. In permanent daylight conditions, wind speed is the main parameter determining diurnal warming events. Diurnal warming free conditions have been defined by wind speed above  $10 \text{ ms}^{-1}$ . This very conservative limit is above the values commonly used ( $6\text{-}7 \text{ ms}^{-1}$ ) but was deduced from analysing OSTIA biases as a function of wind.

The METOP-A prototype has been run with this drastic BT adjustment condition in the Arctic from December 2011 till November 2012. Fig 4 presents the validation results on the corresponding daytime MDB of: the operational algorithm, the bias corrected operational algorithm and the optimal regional NLC determined on the 5 year MDB, as a function of latitude. The OSTIA validation results are also presented for comparison. The bias corrected algorithm shows improved statistics with respect to the operational one; the regional optimal algorithm shows promising results although valid for very limited latitude bands. OSTIA shows a negative bias which did not propagate to the bias corrected algorithm thanks to the wind filtering in the BT adjustment processing.

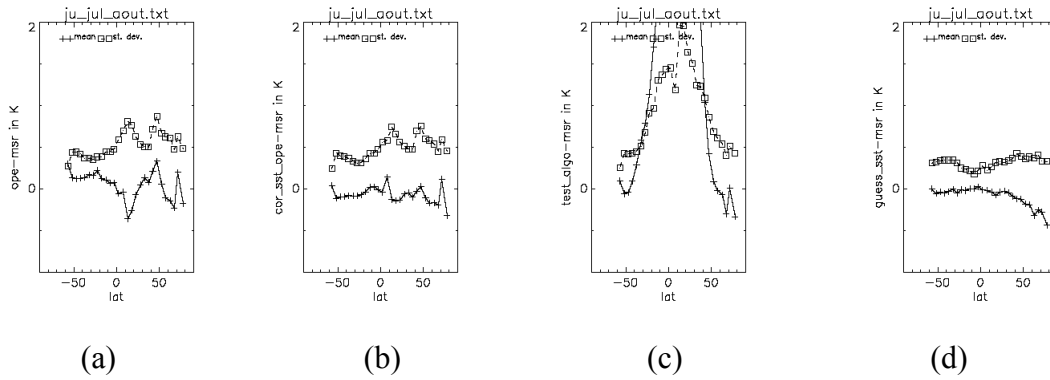


**Fig 4:** Bias and standard deviation as a function of latitude for: a) the operational algorithm; b) the bias corrected operational algorithm; c) the optimal regional; d) OSTIA

### 2.3 Arctic SST algorithms validation results (Jacob Høyer, DMI)

Arctic Ocean is a challenging region for satellite SST retrieval, because of persistent cloudiness, presence of sea ice, complex atmospheric conditions, and extended periods with constant illumination conditions (daytime, night time and twilight). It is also a region where very few in-situ measurements are available. In addition, most of them are concentrated in Nordic Seas and Barents Sea (Fig 5), making validation results not representative of inner Arctic.

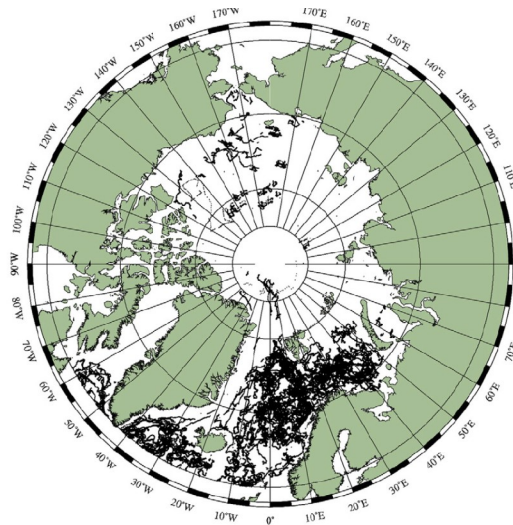


**Fig 5:** Coverage of in-situ SST measurements from drifting buoys North of 60 N.

Nevertheless, 6 operational NRT satellite SST products have been validated at DMI against available in-situ measurements (AATSR, METOP-A/AVHRR, NAVOCEANO GAC, AMSR-E, MODIS Aqua and Terra), and statistics have been produced against various parameters. Most of these products show in the Arctic larger errors than in other regions of the world, and significant biases with a dependency upon solar zenith angle (Fig 6) and total water vapor content.

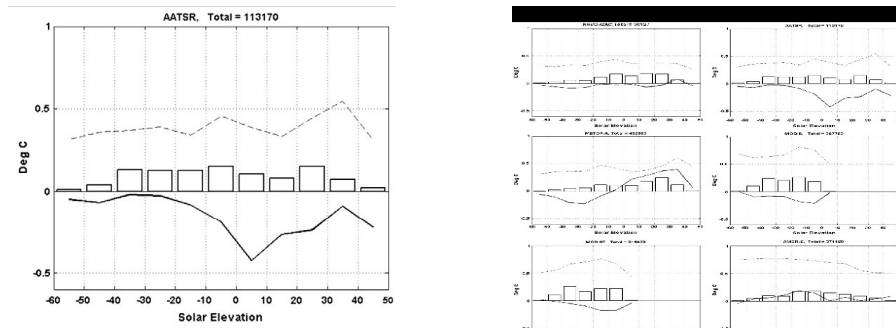


**Fig 6:** Mean (continuous line) and standard deviation (dotted line) of the satellite minus in-situ SST differences in the Arctic as a function of solar elevation for operational NRT AATSR (left) and METOP-A/AVHRR (right) products.

In the framework of the first phase of ESA’s SST CCI project, regional daytime and night time algorithms for SST retrieval from AVHRR on board NOAA-17, 18, 19 and METOP-A satellites (2006-2010) have been derived and their performances have been compared with global algorithms, on an in-situ test data set independent from the training data set. In most cases, regional algorithms are found to improve the retrieved SSTs in the Arctic compared to global algorithms in terms of bias, the largest improvements being for daytime algorithms. When looking at the characteristics of the atmospheric profiles in the Arctic, satellite SST errors (i.e. departures between satellite derived SSTs and in-situ SSTs) seem to be slightly correlated with temperature inversions (defined as the air temperature difference between 900 hPa and surface). Such temperature inversions are found to happen much more often in the Arctic than in the Southern Ocean.

The long term series of satellite SST products (L2P and L3U), which have been reprocessed by ESA’s SST CCI project, have been validated in the Arctic (latitude > 60 N) and in the Southern Ocean (latitude > 50 S), using the CCI Multi-sensor Match-up Data Base. These reprocessed satellite SST products were retrieved from ATSRs (ATSR-1, ATSR-2 and AATSR) and AVHRRs (NOAA-12, 14, 15, 16, 17, 18 and METOP-A) measurements, using an Optimal Estimation method. Median and standard deviation of the satellite minus in-situ SST differences were computed. Overall biases (without separating daytime and night time cases) both in Arctic and Southern Ocean are equal or smaller than 0.1 K in absolute value for all satellites, except NOAA-18. Standard deviation is always larger in Arctic than in Southern Ocean. The variation of these differences has been studied as a function of solar zenith angle and total water vapour content in both Arctic and Southern Ocean. In the Arctic, AVHRRs generally show a cold bias during summer (Fig 7), and for all instruments a bias dependency on total water vapour is found (cold bias at high values).

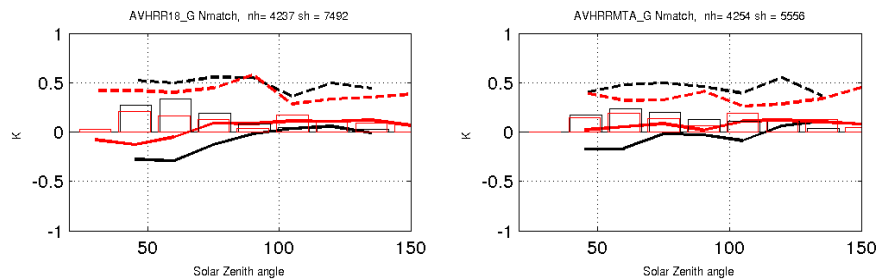


**Fig 7:** Mean (continuous line) and standard deviation (dotted line) of the satellite minus in-situ SST differences in Arctic (black) and Southern Ocean (red) as a function of solar elevation for CCI NOAA-18 (left) and METOP-A (right) AVHRR products.

## *2.4 Arctic SST retrieval in the CCI project (Owen Embury, University of Reading)*

The main objectives of the first phase of the SST CCI project was to produce a long series (August 1991 – December 2010) of satellite infra-red SST observations, compliant with the climate community requirements, and combining the accuracy of the (A)ATSR instruments with the coverage of the AVHRR instruments. This was obtained by retrieving SST through an Optimal Estimation (OE) method, cross-referenced to ARC (A)ATSR SST, and by performing a diurnal variability adjustment, to report SSTs at a standard Local Solar Time (10:30 AM and PM) and a standard depth (20 cm). All SST products are provided with uncertainty estimates, in a netCDF4 GDS2.0 compliant format. The (A)ATSR products were processed using a Bayesian cloud screening, and delivered as L3U products at 0.05° resolution. The AVHRR products were processed using the CLAVR-X cloud screening plus an ad-hoc ice detection, and delivered as L2P products at GAC resolution.

The current Bayesian cloud detection used for (A)ATSR instruments can be considered as a Bayesian “clear-sky” detection scheme, based on infra-red channels only (because of ARC software heritage), and hence has problems in detecting conditions which look like clear-sky in infra-red, namely sea ice or fog. In the second phase of the SST CCI project, the following potential improvements are envisaged: addition of sea ice and fog extra classes, use of visible channels, and revision of prior SST error assumptions in Arctic areas. The OE SST retrieval is based on a Maximum A Priori (MAP) formulation, by setting the prior SST error at a high value (5 K), to reduce the influence of prior SST on the retrieval. The Quality Control (QC) of retrieved SSTs is based on a  $\chi^2$  calculation, which is similar to  $P(\text{obs} \mid \text{clear})$  in Bayesian cloud detection. An additional QC check is performed to remove SSTs < 271.35 K (not applied in pre-release data).

The CCI datasets have been compared for the years 2008 and 2010 in the Arctic with the following SST products, under the form of 5 day composite images: Pathfinder v5.2, ARC v1.1.1, AMSR-E v7 and OSTIA.

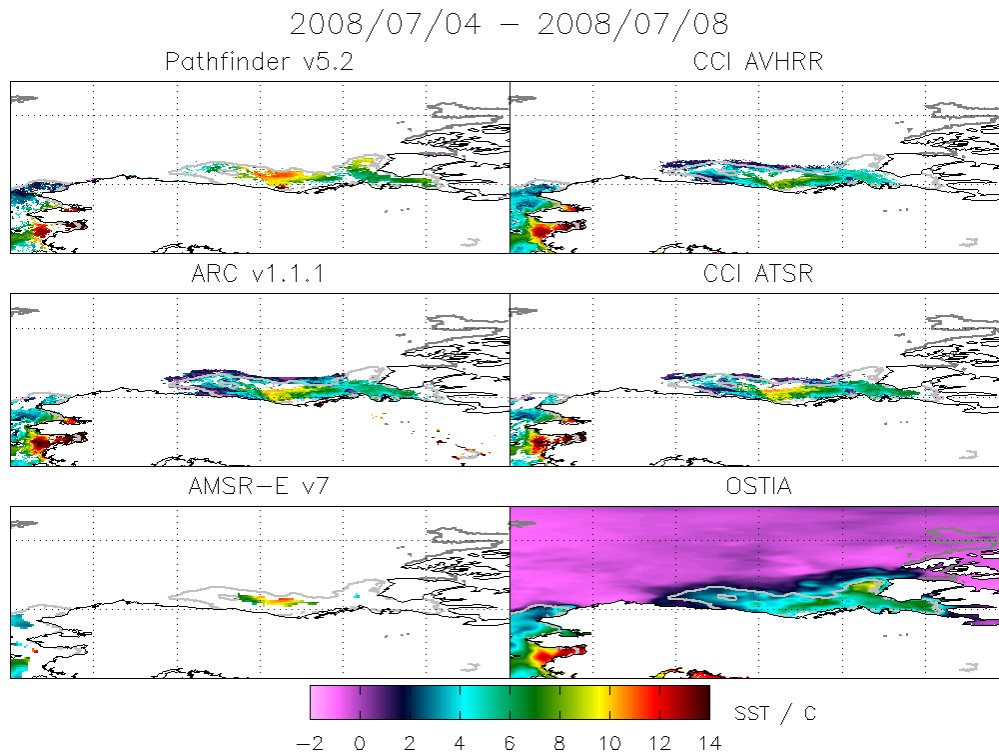


**Fig 8:** Example of 5 day composite SST images in the Beaufort Sea area, from 4 to 8 July 2008. The 15 % and 85 % contour lines from the OSI SAF sea ice concentration product are superimposed in grey.

In Fig 8, a difficult case example in the Mackenzie River outflow region is shown, where high SSTs (up to 12° C) are observed in the Pathfinder and the AMSR-E products, but are totally masked in the CCI AVHRR products, and partially in the ARC and CCI ATSR ones. These high values are due to the strong vertical stratification at the ocean surface because of fresh water. The OSTIA SSTs are much cooler (around 4° C), and are probably the cause of the problems in the Bayesian cloud detection and/or the OE QC checks based on the  $\chi^2$  calculation, which use OSTIA as prior SST.

### *2.5 Bias in Arctic Ocean SST Retrieval from Metop-A AVHRR (Chris Merchant, University of Reading)*

There is a strong perception that SST retrieval biases are poor in the Arctic. SST retrieval methodologies, which rely on BTs simulations, help to reduce biases in the case of atypical atmospheric profiles. But biases may arise in BTs simulations from forward model errors, biases in NWP outputs used for simulations, and sensor calibration. Moreover, the error covariances of BTs simulations are not well known. The aims of the present study are:

- to assess the significance of biases versus drifters for OSTIA, METOP-A/AVHRR SSTs retrieved using OSI-SAF operational 3-channel coefficients (night time), and METOP-A/AVHRR SSTs retrieved using a naïve implementation of OE,
- to consider two candidate “bias tolerant” approaches for satellite SST retrieval

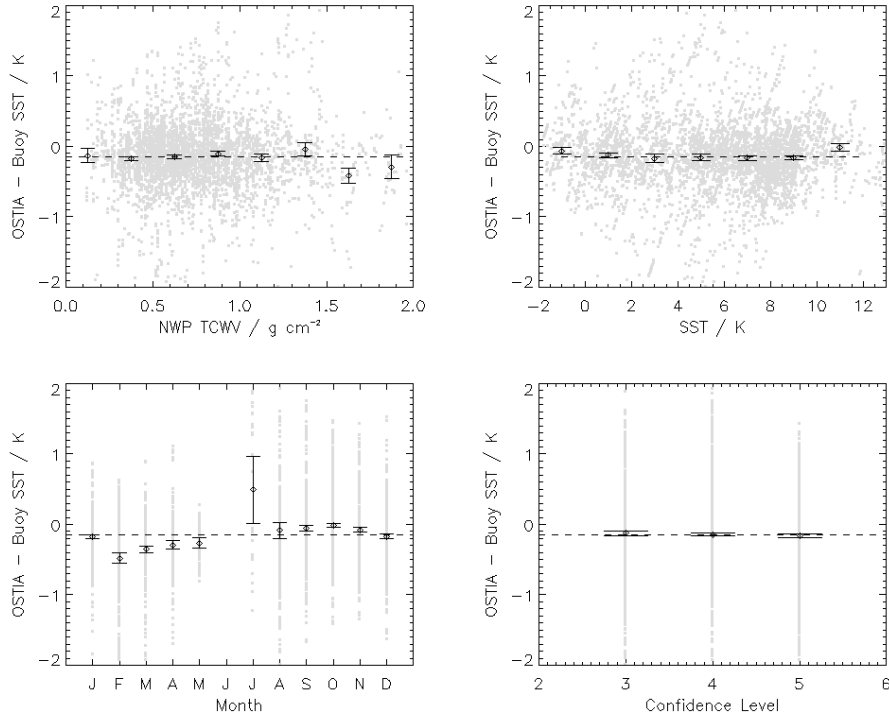


**Fig 9:** OSTIA minus buoy SST mean differences (diamond), as a function of NWP total water vapor content, measured SST, month and Confidence Level. The statistics are based on the one year match-up data set described in the text. Dashed line is the overall mean difference. The bars show 95% confidence intervals on the mean difference, which are calculated using the assumption that errors are independent.

This study is based on a one year match-up data set from OSI SAF over the Arctic (north of  $60^{\circ}$  N), where data have been filtered against buoy blacklist, and for solar zenith angles  $> 90^{\circ}$  (twilight and night), resulting in a total of 4383 matches. The data set includes observed and simulated METOP-A/AVHRR BTs at 3.7, 10.8 and 12.0 microns, their simulated jacobians against surface temperature and total water vapor content, angles, OSTIA “foundation” SST etc.... The mean and standard deviation of OSTIA minus drifters differences, obtained on this data set, are  $-0.14 \pm 0.51$  K (median and robust standard deviation:  $-0.14 \pm 0.34$  K). However, OSTIA is not independent from drifters measurements, which are assimilated in OSTIA. Fig 9 shows the OSTIA minus buoy SST differences, as a function of NWP total water vapor content, measured SST, month and Confidence Level, as well as the corresponding 95% confidence intervals. There is a statistically significant dependence of the mean differences on the month of the year, and to a lesser extent on the total water vapor content for values  $> 1.3$   $\text{g cm}^{-2}$ , and on measured SST for values  $> 10$  K, but neither on latitude, satellite zenith angle nor solar zenith angle (not shown).

The same statistics, derived for night time OSI SAF operational METOP-A/AVHRR SSTs, on the same date set, show significant dependencies of the mean satellite minus buoy SST differences on all variables, except Confidence Level. When applying the simulated bias corrections, these dependencies are generally significantly reduced, but an overall mean difference of  $-0.26$  K (median:  $-0.21$  K) is found, which is not fully understood (are the retrieved corrected SSTs supposed to represent skin or sub-skin SSTs ?).

The OE method assumes that there is zero bias in BT simulation relative to observation, and that we have good estimates for the prior error co-variances ( $S_a$ ), the sensor noise and the forward error model co-variances ( $S_e$ ). These assumptions are of course not true, in particular the zero bias assumption (hence the efforts on BT bias adjustment). A “naïve” implementation of OE, with no BT bias adjustment, is first tested, resulting on the same match-up data set in a mean and standard deviation of the difference of  $-0.07 \pm 0.58$  K (median and robust standard deviation:  $-0.01 \pm 0.40$  K). When using in addition the OSI SAF BT bias adjustment prior to OE retrieval, the overall error statistics are almost unchanged (mean and standard deviation:  $-0.04 \pm 0.58$  K, median and robust standard deviation:  $0.02 \pm 0.39$  K), the main improvement being for the Confidence Levels equal to 3.

Two approaches for “bias-tolerant” retrievals are then studied. The first one is the Modified Total Least Squares (MTLS) method, developed by Prabhat Koner (NOAA), who successfully applied it for GOES-12 SST retrieval using 3.7, 11 and 13 microns channels without any BT bias adjustment, when an OE retrieval without BT bias adjustment was reported to give bad results. The MTLS method is based on a gain matrix, which includes a variable regularization parameter  $\lambda$ , depending on how “good” is the match between observations and simulations. When applied on the OSI SAF match-up data set for METOP-A/AVHRR data, the MTLS method, which doesn’t use any BT bias adjustment, results in a mean and standard deviation of the difference of  $-0.04 \pm 0.58$  K (median and robust standard deviation:  $-0.00 \pm 0.39$  K). When looking at the mean differences dependency on various parameters, significant dependencies are found on almost all them, except satellite zenith angle (not shown). The second approach is based on a “bias-aware” OE formulation (MAPBA), where mean differences between observed and simulated BTs are first estimated, with a stratification by Confidence Levels (3, 4 and 5). Then, the co-variances of the de-biased observed minus simulated BTs differences are calculated, and taken into account in the  $S_e$  variance/co-variance matrix, which represents instrument noise plus forward model error. When applying this method on the OSI SAF match-up data set, a reduction in error standard deviation is obtained (mean and standard deviation:  $0.02 \pm 0.53$  K, median and robust standard deviation:  $0.05 \pm 0.37$  K). Fig 10 shows the dependency of the mean differences between MAPBA satellite retrievals and buoy SSTs on NWP total water vapor content, measured SST, month and Confidence Level. In terms of dependencies, there is no clear improvement of the MAPBA method compared to the MTLS method, except for the dependency on Confidence Level.

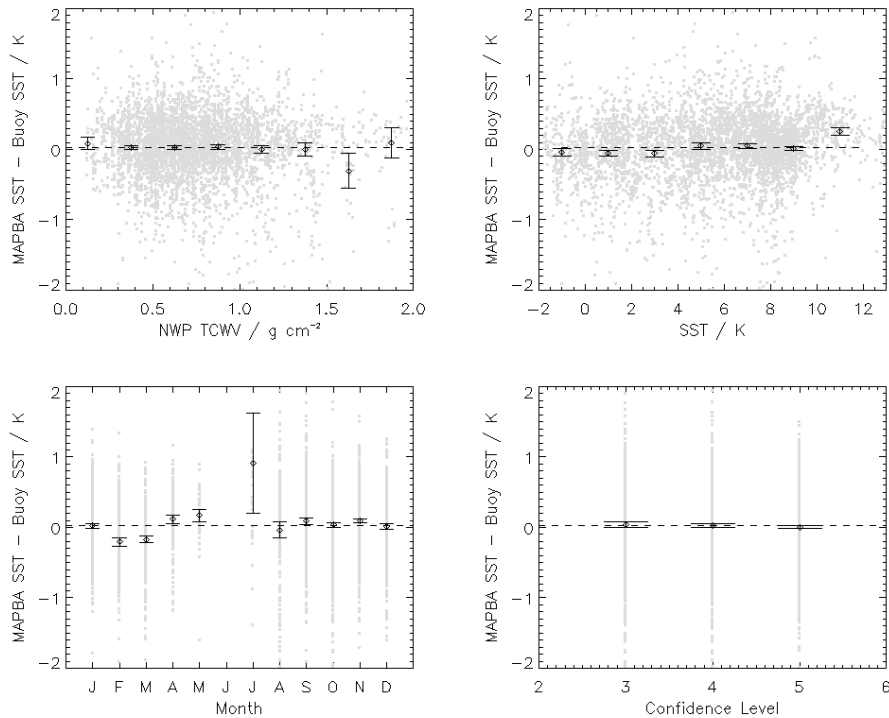


**Fig 10:** MAPBA (METOP-A/AVHRR SSTs retrieved using the “bias aware” OE approach) minus buoy SST mean differences (diamond), as a function of NWP total water vapor content, measured SST, month and Confidence Level. These statistics are based on the same data set as in Fig 9.

## 2.6 Summary of open issues and potential solutions from session 1

### a) Cloud and ice detection (S. Eastwood/O. Embury):

- Problems: the separation between water, clouds and ice in polar regions is very difficult using infra-red channels only; this will be the case anyway in night time conditions. As a consequence, the ability and the errors in water/cloud/ice separation will always be very dependent on illumination conditions (day time, night time and twilight). The Bayesian cloud detection scheme used in the CCI project, which is based on infra-red measured and clear-sky simulated brightness temperatures, is very vulnerable to large errors in the prior SST used (OSTIA up to 10 K too cold in some cases in the Arctic)
- Solutions: in the second phase of the project, the CCI Bayesian detection scheme will be upgraded by adding an ice class, and by changing the assumptions about prior SST errors in coastal regions. As a more general consideration, the advantage of the Met Norway Bayesian classification scheme is that it doesn't rely on clear-sky simulated brightness temperatures, but on “features” in the satellite measurements (for instance combinations of different channels), and hence doesn't need any prior SST field.

### b) Use of NWP-based radiative transfer simulations in the Arctic (P. Le Borgne):

- Problems: the main problem encountered by the OSI SAF in the preparation of its new METOP/AVHRR SST processing chain is the adjustment of simulated brightness temperatures, which are used for SST corrections. In the Arctic, radiative transfer simulations based on OSTIA “foundation” SSTs are very difficult to compare with observations, since “foundation” SST is very scarcely observed from space in low/medium wind and permanent solar illumination conditions.
- Solutions: the current approach tested in the Arctic for simulated brightness temperatures adjustment is to use a drastic wind filtering. However, this approach is somewhat fragile, and CMS will test regional high latitude algorithms as a back-up solution. This will require the building of an atmospheric profile data set adapted to Arctic conditions. CMS and DMI will also compare their results concerning METOP-A/AVHRR SST biases, derived from their respective SST correction methods.

c) SST algorithms in the Arctic (J. Hoyer):

- Problems: all satellite SST products ((A)ATSR, AVHRRs and AMSR-E) have generally larger errors in the Arctic, compared to Global and Southern Ocean performance, and their biases generally depend on solar zenith angle and total water vapour content. Regional AVHRR SST algorithms, fitted to Arctic conditions, can decrease biases, the largest improvements being found for day time algorithms. In the Arctic region, the cases where the largest satellite SST retrieval errors (compared to buoys measurements) are found, correspond to more humid and warmer atmospheric profiles than for the cases with small errors.
- Solutions: the relationship between satellite SST retrieval errors and atmospheric profiles in the Arctic will be further explored, using the CCI Multi-sensor Match-up Data Base. Additional in-situ SST measurements for validation in the Arctic will be looked for, for instance the ones collected during research campaigns.

d) Physics-based SST retrieval in the Arctic (C. Merchant):

- Problems: errors in radiative transfer simulations can arise from surface temperature errors, Radiative Transfer Model (RTM) errors and NWP profiles errors; little information is available on the magnitude of these error sources in the Arctic conditions. In addition, inter-channel co-variances of RTM errors are not well known.
- Solutions: new “bias tolerant” approaches for SST retrieval will be further explored; one of them is the Modified Total Least Square method, proposed by P. Koner (NOAA). In the OE framework, another approach is proposed by C. merchant, based on an empirical mean Brightness Temperature (BT) bias adjustment, and an empirical forward model error co-variance matrix, which reflects any correlated BT bias components.

### 3. Summary report of session 2: Analysis in the Arctic (Emma Fiedler, Met Office, Jacob Høyer, DMI, Jonah Roberts-Jones, Met Office).

The L4 products that were presented in this session (OSTIA and DMI-OI) share similar difficulties in the analysis of Arctic SST. These difficulties are described below, along with suggestions for overcoming problems. A summary is provided at the end.

Although many issues and problems were described in this session, it should be noted that overall the performance of L4 analyses in the Arctic is good. The validation of the DMI L4 analysis resembles the L3 input validation, both spatially and temporally, which means the analysis procedure itself is not introducing any major errors. It was also shown that observations have plenty of influence in the analysis. Drifter observation-minus-background statistics over one month show the new implementation of OSTIA with updated background error covariances has improved the Arctic SST, which now has an RMS error of 0.45 K compared to 0.58 K for the old implementation of OSTIA.

Since the demise of the AATSR instrument, an important general issue affecting Arctic SST analyses is the current lack of reference quality satellite SST observations to supplement the in situ observation network. Reference data are routinely used to bias-correct the other satellite observations. The planned launch of the SLSTR instrument onboard Sentinel-3 should provide new global reference-quality data or, in the intervening time, data from the VIIRS instrument aboard the Suomi-NPP satellite may prove suitable. OSTIA currently uses a high-quality subset of MetOp AVHRR data (using only nighttime observations close to nadir) as a reference dataset. However, this approach is problematic in the high latitudes around the summer solstice due to lack of nighttime data.

It should be noted that problems in the high latitudes (such as issues with ice and cloud masking) were also present in the AATSR data. A multi-satellite reference approach, which is currently used by the Ifremer ODYSSEA analysis, is being considered for use in OSTIA. However, for this method to be implemented within OSTIA, improvements would need to be demonstrated for the full global SST analysis and not just solely for the Arctic.

The DMI reanalysis in the Arctic showed that the mean monthly differences of the Pathfinder vs. AATSR SST observations were relatively consistent from one year to the next (Figure 1). This indicates that inter-comparisons of the monthly biases between the different L4 products could help in determining the optimal reference sensor. This is particularly important for the Arctic, as a lack of in situ data makes the assessment of different bias correction options difficult.

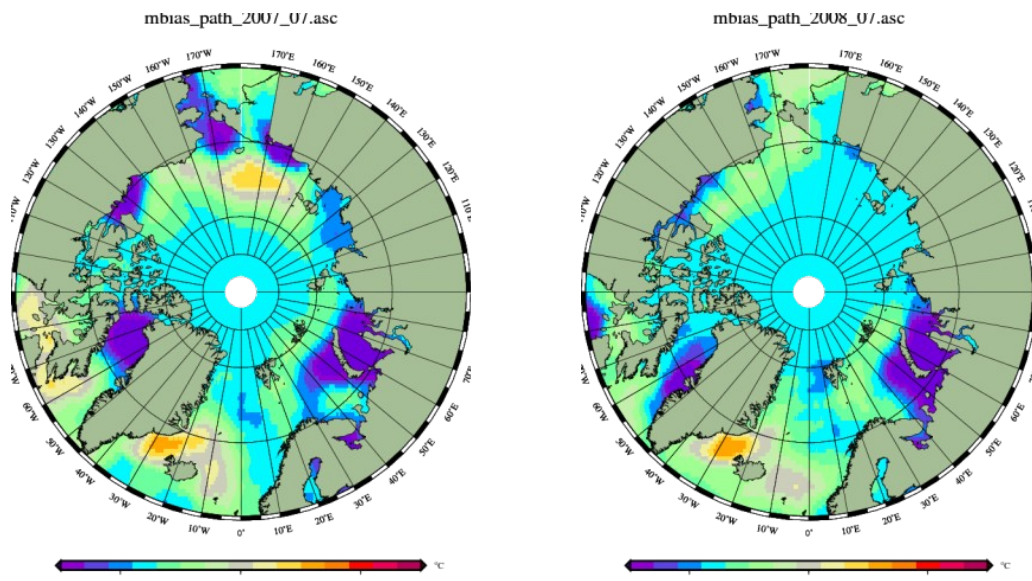


**Figure 1:** Mean monthly SST difference of Pathfinder vs AATSR for July 2007 (left) and July 2008 (right).

Although some in situ observations are available for the Arctic region, mostly from drifting buoys, they are spatially sparse. As well as only providing sparse reference data, this low volume of in situ data makes it difficult to identify regional biases in analyses, using traditional validation methods (e.g. observation-minus-background). More in situ observations are available from scientific research projects and field campaigns, but these are typically not included in validation exercises due to differing data formats and unknown error characteristics.

As well as the overall low number of observations available for assimilation by Arctic analyses (e.g. due to persistent cloud cover) it was also shown that there is an issue with lack of agreement between observations from different satellite and in-situ instruments in this region. For example, Figure 2 demonstrates that drifter observations are biased compared to the OSTIA analysis, by around 0.2 K, despite being used as a reference dataset. The analysis also uses a high quality subset of MetOp AVHRR data as a reference, as mentioned above, and hence there must be differences between the in situ and MetOp AVHRR datasets.

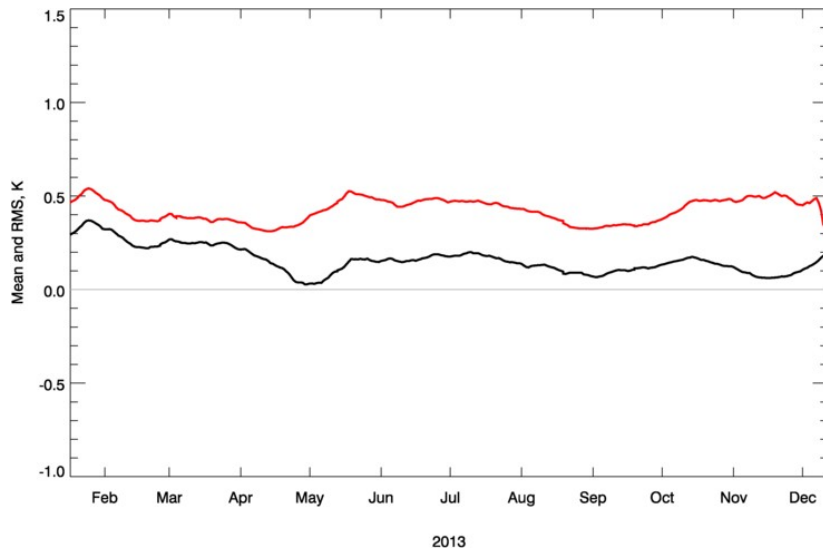


**Figure 2:** Drifter-minus-Analysis in the Arctic region. Black line is bias, red line is RMS error.

The persistent cloud cover in the Arctic means SST observations obtained from microwave instruments are useful. In addition, the errors on microwave retrievals have been demonstrated to be independent of errors on infrared SST retrievals. There has been a data gap in available global microwave data since measurements from the AMSR-E instrument ceased, but observations from the new AMSR-2 instrument are now becoming available and should be made use of. However, there are no microwave observations in coastal regions or in the Canadian Archipelago, due to the large footprint of microwave instruments.

It was shown for both the DMI and OSTIA analyses that the treatment and inclusion of information near the ice edge is challenging. Sea ice concentration and SST analysis are two very different datasets. Achieving consistency between the two can be difficult, particularly where very strong SST gradients exist. The current method of SST relaxation to freezing under ice in OSTIA does not always achieve a realistic level of consistency (alteration of minimum ice concentration and timescales for SST relaxation to freezing have little effect).

Recent updates to the OSTIA system, which have improved Arctic SSTs overall, have reduced the level of consistency between the ice and SST. Length scales at the ice edge can spread SST increments too far under the ice, causing inconsistencies between the OSTIA SST and ice concentration (Figure 3). In order to prevent this, the approach of assimilating pseudo-observations under ice of e.g.  $-1.8^{\circ}\text{C}$  based on ice concentration has been considered, an approach already implemented by DMI (and CMC). However, DMI has encountered the problem of cold increments from the under-ice pseudo-observations being spread too far into the open ocean, leading to a cold bias along the ice edge. An anisotropic, ice edge dependent assimilation length scale, which varies daily, would help both problems. This should be possible in the future for OSTIA, using the new NEMOVAR assimilation scheme currently being implemented, and performed in a similar way to the method being planned for use along SST fronts.

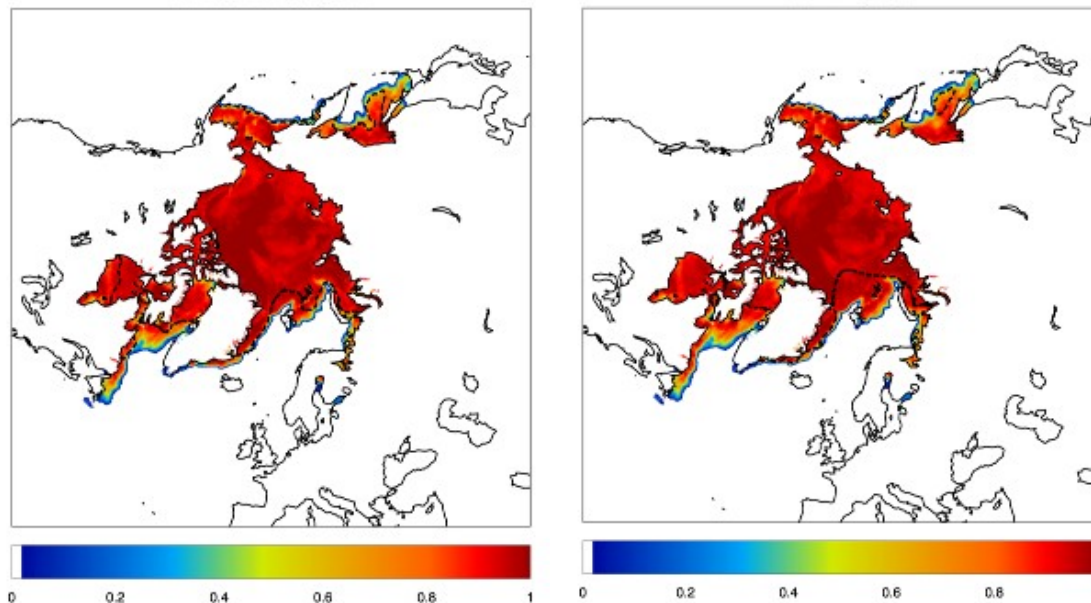


**Figure 3:** OSTIA sea ice fraction and freezing SST (dashed black line) using old background error covariances (left) and new (right) for the Arctic, on 26 March 2012.

Use of an ice assimilation method in OSTIA would also be beneficial. Currently, for OSTIA, the ice concentration is essentially a regridding of the daily OSI-SAF ice concentration product. OSTIA has the capability to perform spatial interpolation across ice data gaps within the sea ice region (for example, at the pole hole), but across the ice edge this method produces poor results. A solution in the short-term to spatial gaps in the data could be to set up a temporal interpolation or to persist the ice field from the previous day. However, a sea ice assimilation would fix this problem.

In order to maintain consistency, balance relationships between the SST and ice concentration must be known. It is likely that freezing SST and sea ice relationships differ in melt and freezing seasons. Assessment of these relationships could be achieved using long timeseries of SST and ice (e.g. from reanalyses) or comparisons to FOAM or other 3-D models. This would allow better understanding of SST characteristics around sea ice. These relationships could also be used to implement statistical methods for improving consistency of the sea ice concentration and freezing SST. In OSTIA it is assumed that the sea ice concentration is more reliable than SST at high latitudes, and so methods to adjust the SST based on the ice should be used, rather than vice versa.

The use of a salinity climatology for freezing temperature could help to improve issues of consistency between ice and SST, although, for example, the Met Office NWP team (and other users of OSTIA) treat freezing temperature as a single value of  $-1.8^{\circ}\text{C}$ , so this aspect would need to be considered before any changes could be implemented.

Inter-comparison of analyses is important as it allows us to share ideas and assess different methods used. In this way, the successes or problems of a particular method can be highlighted and thus it is useful to have variation in methods between different products. The GMPE (GHRSSST Multi-Product Ensemble), which is currently used for NRT comparison of different L4 products, could be used to compare different analysis methods. The same input data and same ice mask could be used, providing a clear comparison of the analysis systems

themselves. This could be particularly useful for examining the regional (high latitude) performance of new assimilation schemes, e.g. NEMOVAR. An inter-comparison of different sea ice concentration products would also be desirable.

Results from a comparison using GMPE of various NRT L4 analyses in the high latitudes were shown. It was demonstrated, not unexpectedly, that all the contributing analyses display the largest variation from the GMPE median in the high latitudes. The magnitude of this variation differs interannually, with large variation between analyses. To assess this variation, a description of the methods used by different centres to produce their sea ice and high latitude SST analyses would be useful, particularly those methods used to achieve consistency between the ice and SST data.

Large diurnal warming events have previously been observed in the Arctic. A 3-hourly diurnal version of OSTIA, using a diurnal variability model on top of the foundation temperature currently produced, is being developed. It would be interesting to examine case studies of Arctic diurnal warming events using this new diurnal implementation.

## SUMMARY

- Overall, L4 analyses in the Arctic are good
- For improvements, need quality satellite reference dataset and more in situ for reference and/or validation
- Arctic observations don't always agree with each other
- Largest differences between global NRT L4 SST analyses are in the high latitudes
- Persistent cloud cover in Arctic means use of microwave data is important
- Improvement of analysis performance and ice/SST consistency near the ice edge is a priority
- Adjustment of correlation length scales dependent on position of ice edge useful
- Freezing SST/ice concentration relationships should be investigated, for statistical or ice assimilation methods
- Diurnal warming events in the Arctic could be investigated using L4 analyses

### 3. Summary report of session 3 : SST variability in the Arctic (S. Eastwood, Met Norway)

The third session of the EarthTemp Arctic SST workshop dealt with SST variability in the Arctic, with focus on the SST in the Marginal Ice Zone, diurnal warming and vertical temperature profiles. The next sections contain short resumes of each presentation.

#### *3.1 SST variability in the Arctic (Jacob Hoyer, DMI)*

SST retrievals are challenging in the Marginal ice zone, due to the presence is sea ice, large SST gradients and atmospheric conditions. Several definitions of marginal ice zone exist but the one applied here is given by Wadhams (1986) : "that part of the ice cover which is close enough to the open ocean boundary to be affected by its presence".

The marginal ice zone show very large seasonal changes in the size and location. is seasonally very varying and covers large areas of the Arctic ocean. Figure 1 below show the climatic variability of the sea ice concentration fields in the months of September (left) and March (right). The highly variable areas outline the Marginal Ice Zones during these months.

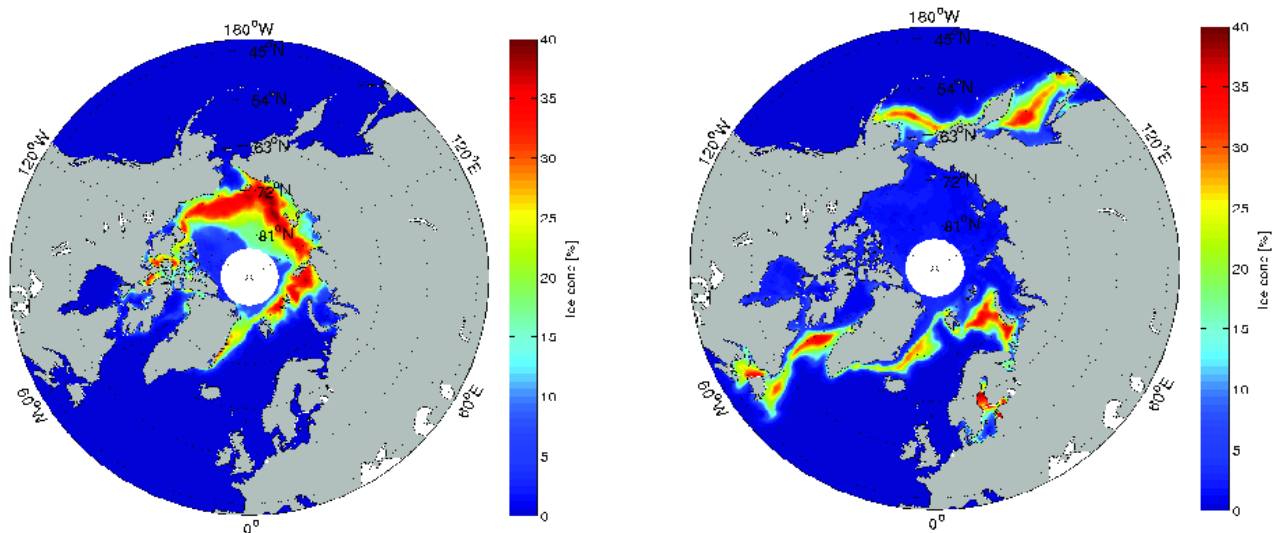


*Figure 1: Standard deviation of Sea ice concentration for September (left) and March (right). The data set used is the Ocean and Sea ice SAF reanalysis covering the years 1979-2009.*

Few studies have focused upon the quality of the SST retrievals in the MIZ. The presentation highlighted some areas where a potential for more work is available. The work includes collection of MIZ data sets and the validation and characterization of the individual retrievals in the MIZ. The operational focus will be on the DMI SST-MIZ-IST data products from Metop-A, whereas the climate data records of SST (from Pathfinder and the ESA CCI project) will be used to validate and relate SST and Sea ice concentration fields for different regions and seasons.

The work within the MIZ will consist of following tasks:

- Determine the SST signal within MIZ for different ice concentrations, for different regions and seasons
- Compare SST and Metop-a in MIZ
- Determine the impact of SST gradients in MIZ on SST performance
- Collect in situ observations in MIZ through field campaigns
- Verify and update MIZ algorithm in Metop-A
- Implement the SST versus Sea Ice concentration relationships in the DMI-OI level 4 SST products for the Arctic.

### 3.2 Diurnal warming in Lake Vänern (Steinar Eastwood, C. Luis and L-A. Breivik, Met. Norway)

#### Introduction

The Norwegian Meteorological Institute has deployed a moored buoy (actually a buoy of drifting type with mooring) in Lake Vänern in Sweden. The purpose of the deployment was to validate OSI SAF SST products in this lake and to study diurnal warming. Lake Vänern is the third largest lake in Europe, position at 59N at an altitude of 44m. This is fairly shallow lake with average depth of 27m and quite turbid waters (Secchi-depths of about 3-5 meters). The buoy is equipped with a standard thermistor and GPS and transmits every 30 minutes through Iridium. The temperature is measured at about 20cm depth. Below the buoy there were six additional temperature loggers at different depths to measure the temperature profile in the upper 2.4 meters. The buoy was deployed at the same position from 3rd May to 15th October. The buoy setup is shown in Figure 6.

A data set has been built with the buoy data and all the temperature loggers collocated in time. To better be able to study the diurnal warming events in Lake Vänern wind speed from the regional NWP model HIRLAM (12km resolution) have been interpolated to the buoy location and been added to the data set.

#### Results

The data from the buoy showed frequent cases of diurnal warming from end of May to mid September. A few days also had very strong diurnal warming, with a particular strong case on 1st June with an observed difference of 6°C between morning and evening. The 1st June case was actually three days in a row with significant diurnal warming at the buoy location, as shown in Fig. 3. The warming during

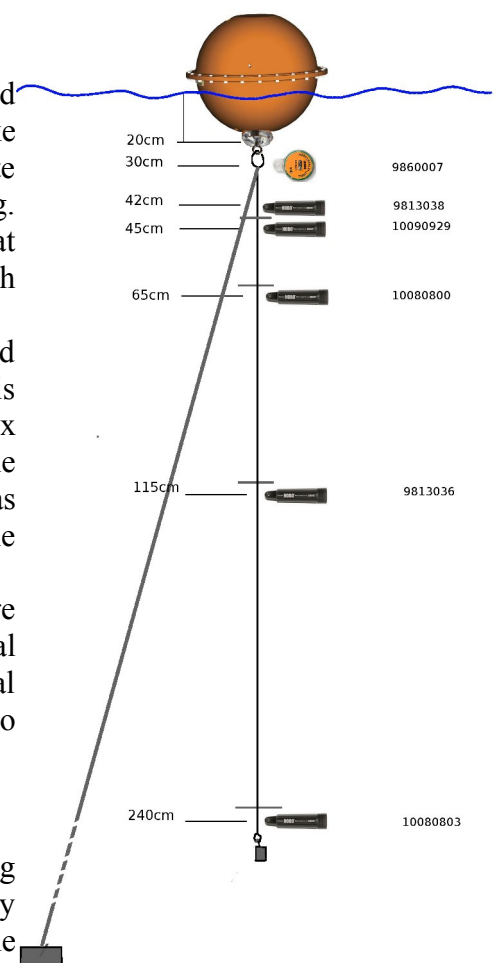


Figure 2: Lake Vänern buoy setup.

each day is accumulated at depths down to somewhere between 1.1 and 2.4 meters, allowing a stronger stratification to build up and the diurnal warming to start at a higher level each morning. The diurnal warming event occurred during a period with low wind speed, between 0 and 3 m/s for most of the period.

The set of temperature measurements at different depths were used to study how the diurnal warming change differs at different depths. Fig 4 shows the mean diurnal warming as difference from the minimum temperature between midnight and 06:00 for all days with a diurnal warming above 1.0°C. The diurnal warming amplitude decreases with depths. In addition, there is a shift in when the amplitude maximum occurs, with the amplitude occurring later at day at deeper layers.

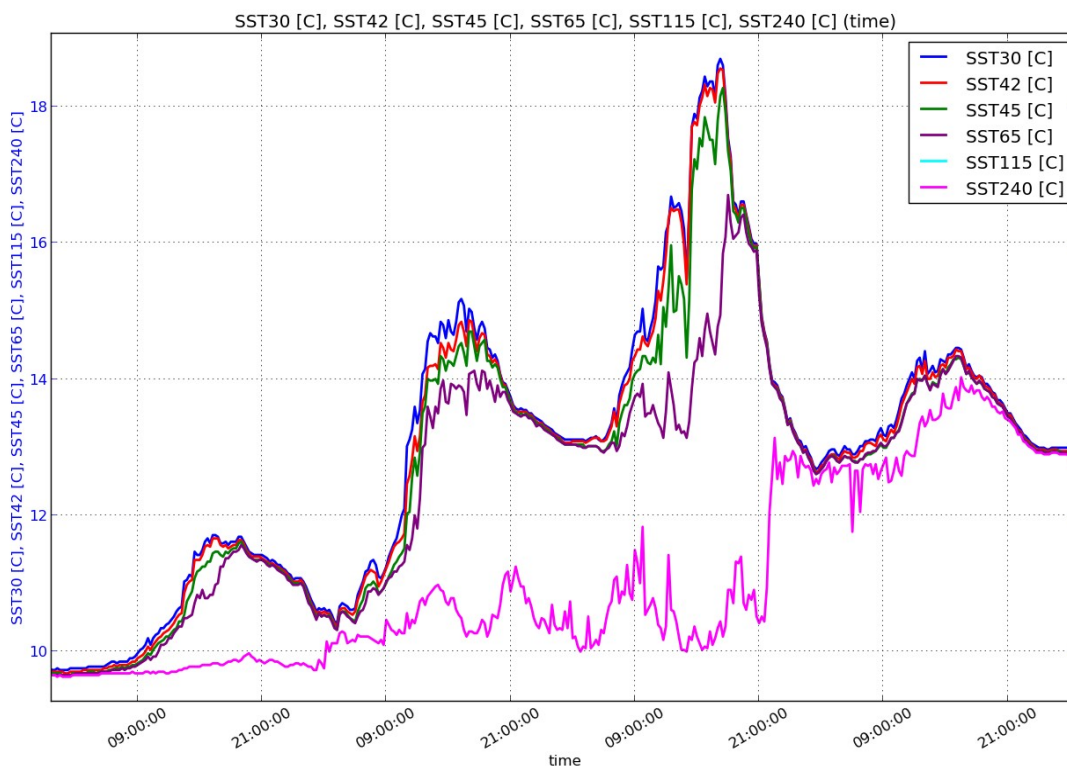


Figure 3: Temperature at different depths during the three day diurnal warming event ending at 01-06-2013.

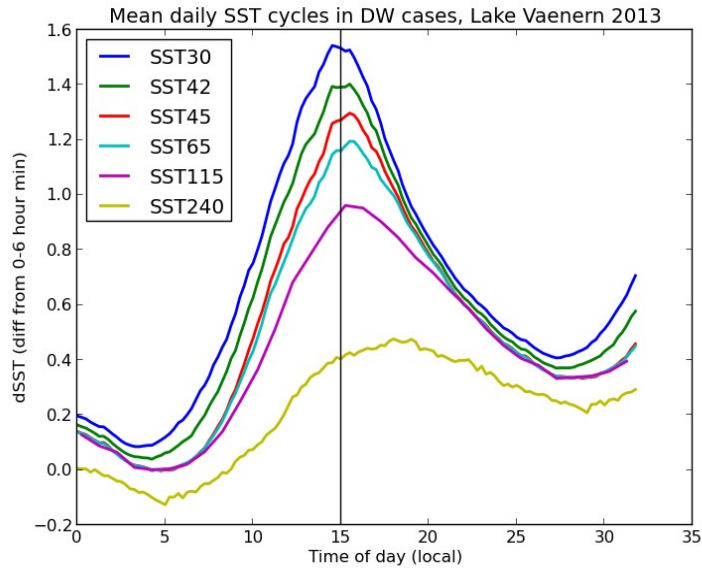


Figure 4: Mean diurnal warming profile for Lake Vänern buoy.

### Conclusions and further work

The buoy deployment in Lake Vänern has shown that this is a good spot for performing diurnal warming experiments at high latitudes, where instrumentation can be more easily deployed. The data will be very useful to better understand the mechanisms for diurnal warming at high latitudes, and further work on this data set is expected at MET Norway and CMS, with the intension of publishing a paper before summer 2014.

The buoy will be deployed again in April 2014, with some modifications. Additional temperature loggers will be placed at 5 and 10 meters, and a wind speed anemometer with logger will be mounted on the buoy.

### 3.3 Diurnal warming in the Arctic, observations at Meteo-France/CMS (Sonia Péré and Pierre le Borgne, M-F/CMS)

#### Introduction

MF/CMS has been studying short term SST variability in the Arctic Ocean for several years (Eastwood et al, 2011). The specificity of Arctic summer (there is no true nighttime period in June July) led us to investigate the definition of diurnal warming, and in particular the definition of diurnal warming amplitude. In mid latitudes (typically, the Mediterranean sea), diurnal warming are closed cycles in which evening temperatures are close to those of the previous night. In the Arctic diurnal warming cycles show in general a very strong residual warming at the end of the day (Figure 5a). Solar warming often covers several days, creating

solar warming episodes with warming in daily steps or cycles as shown in Figure 5b. This leads to question the characterization of warming amplitude: should it be evaluated as the difference between the temperature at time  $t$  and the previous night SST or the temperature preceding the warming episode which is likely the foundation SST.

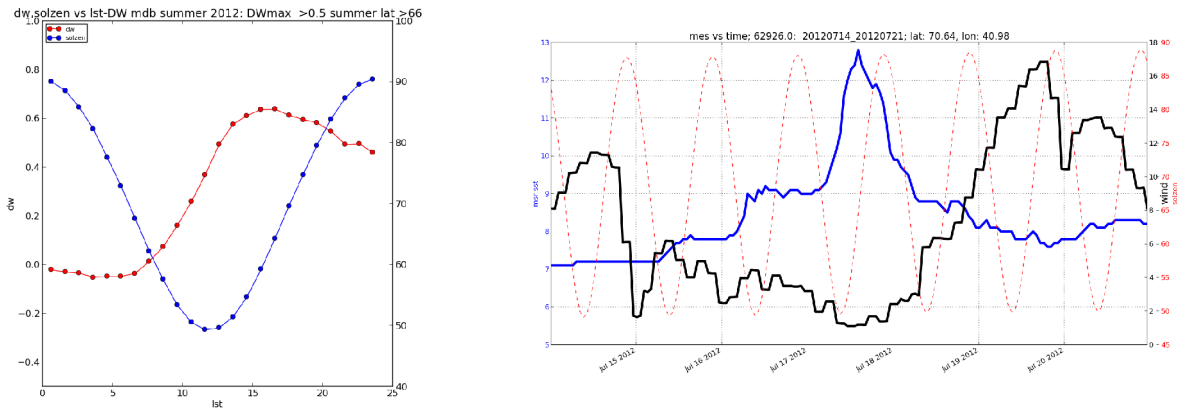


Figure 5: a) Mean diurnal cycle observed on buoy measurements at latitudes above  $66^{\circ}\text{N}$  in summer 2012; b) buoy WMO #62926 measurements from the 14<sup>th</sup> till the 21<sup>st</sup> July 2012 in the Barents Sea (SST in blue, wind speed in black).

This presentation will discuss these options through examples based on buoy observations (next section) or satellite data (section 3). In section 4 we use a 1-D ocean model (Global Ocean Turbulence Model (GOTM) to try to reproduce the observations. In section 5 we conclude and suggest further work.

### Buoys observations

In this section we used data from the CMS “Diurnal Warming MDB” (Péré et al, 2013). This data set includes buoy measurements (and SEVIRI data where available) from June till September 2012. We focus on buoy WMO #62926 which showed a large amplitude signal on the 17<sup>th</sup> of July 2012 by  $70.64^{\circ}\text{N}$  and  $40.98^{\circ}\text{W}$ . The warming amplitude on the 17<sup>th</sup> of July can be either 3.5 K or 5.5 K depending if the reference used is the previous night SST or the foundation (pre-warming episode) SST. The previous night reference SST has been defined has the mean SST after 20 LST the previous day and before 8 LST the same day. As shown on Figure 5b, wind plays a key role in the setting up of warming events. Figure 6a shows that residual diurnal warming disappears for wind above 5  $\text{ms}^{-1}$ . Various trials on buoy data suggested that 7  $\text{ms}^{-1}$  is a safer threshold to identify cases where foundation SST is measurable at surface. Wind above 7  $\text{ms}^{-1}$  are not observed on a daily basis. To obtain a daily value, foundation SST observations (corresponding to wind speed above 7  $\text{ms}^{-1}$ ) have been averaged over 11 days centered on the day in question. The resulting foundation SST estimate seems about satisfactory (Figure 6b).

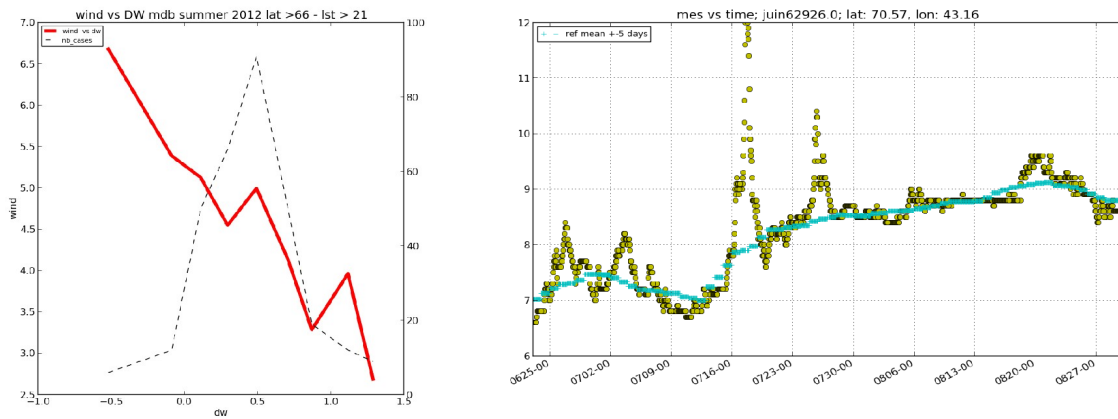


Figure 6: a) Wind speed and residual diurnal warming; b) Buoy WMO#62926 measurement time series (yellow line) and foundation SST (blue line).

### Satellite observations

The same solar warming episode has been analyzed with METOP-A AVHRR derived SST data, which have been produced operationally at CMS for EUMETSAT/OSI-SAF. There is a good agreement between the buoy and the METOP-A SST (Figure 7).

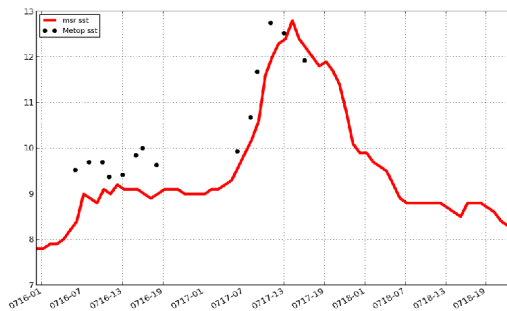


Figure 7: Buoy measurement compared to METOP-A SST time series from the 16<sup>th</sup> till the 18<sup>th</sup> of July 2012.

Previous night and foundation SST can be calculated the same way as defined for the buoy measurements. Diurnal warming amplitudes can be defined in both cases using these two references. Figure 8 shows the difference between METOP-A SST at 11 LST and (Figure 8a) the previous night SST and (Figure 8b) the foundation SST, respectively. The shape and amplitude of the warm spots are significantly different.

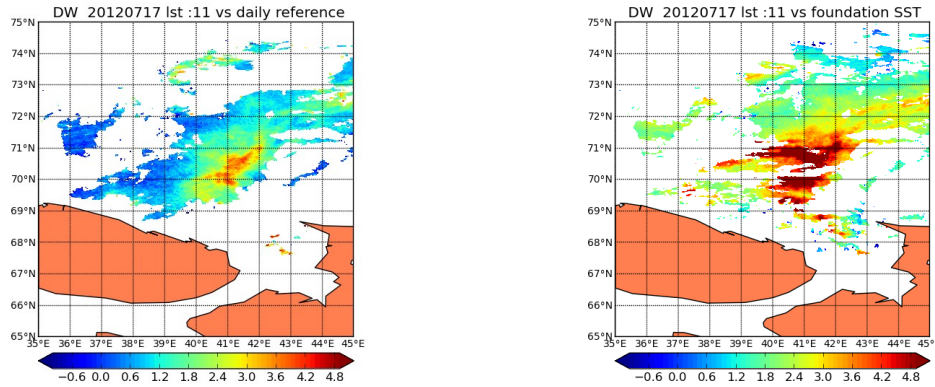


Figure 8: METOP-A derived warming amplitude at 11 LST using as reference: a) the previous night SST ; b) the foundation SST.

Since the difference with foundation SST gives a better representation of the temperatures anomalies generated by a solar warming episode, we tried to map foundation SST in various location (Beaufort Sea, Baffin bay, etc...). The result was disappointing, due to the scarcity of wind speeds above 7 ms-1 in summer Arctic. In July 2012, for instance, the probability for METOP-A/AVHRR of observing the sea surface with a wind speed above 7 ms-1 is in most cases lower than 20% (against 40% in the Aegean Sea).

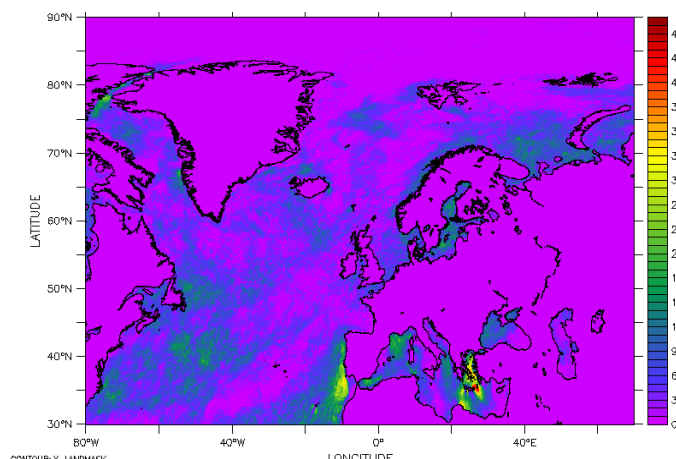


Figure 9: Relative number clear sky cases with wind above 7 ms-1 recorded with METOP-A in July 2012.

### Modeling attempt

It was challenging to reproduce the Barents Sea observed SST variations during the 15<sup>th</sup> to 19<sup>th</sup> July solar warming episode with the Global Ocean Turbulence Model (GOTM). We adopted the GOTM configuration successfully used at CMS in the Mediterranean Sea (Ciani, 2012). Temperature and salinity profiles were initialized with the Levitus atlas data for the location and the day. In a first attempt, we used ECMWF derived wind and surface fluxes as forcing terms of the model. The resulting variations of the SST (Figure 10a) were significantly underestimated with respect to observations. Various tests were made to try to increase the SST variation amplitudes: assigning wind speed to zero on the 17<sup>th</sup> of July (the peak day) or assigning non solar fluxes to zero throughout the period. The only solution to

produce SST variations close to observations was to introduce a density stratification by assigning the first level salinity to zero in the Levitus initial profile (Figure 10b). This assumption is very likely unrealistic, although the Southern Barents sea may be under the influence of low salinity White Sea waters.

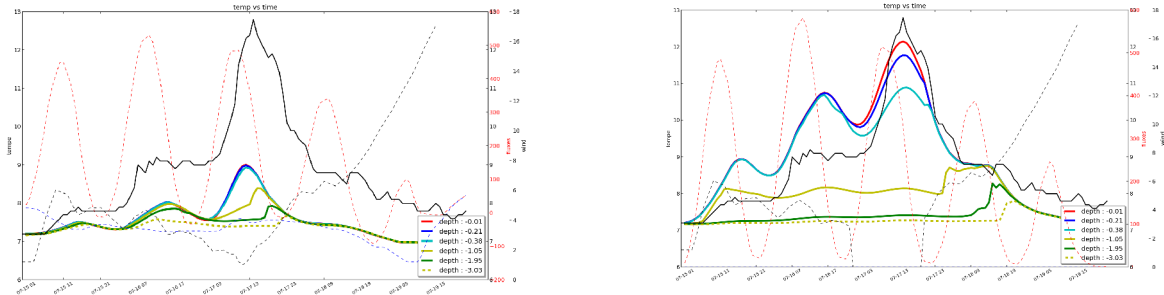


Figure 10: Buoy SST measurements and GOTM outputs: a) with ECMWF outputs; b) with wind assigned to zero on the 17<sup>th</sup>, non solar fluxes assigned to zero and first level salinity assigned to zero.

### Conclusions and future work

Diurnal warming is different in the Arctic from what is usual at lower latitudes. «Solar warming episodes» lasting several days are frequent. “Diurnal warming” during these episodes takes often the form of steps with large residual warming at the end of the day. Diurnal warming amplitudes can be measured either by difference against the previous night SST or the foundation SST preceding the warming episode. This last quantity is thought to be better representative of the amount of heat stored above the «diurnal» thermocline than the daily amplitude. With drifter data, the «solar warming amplitude» over several days can be determined relatively easily. With satellite data, the scarcity of wind >7m/s in clear sky does not permit to determine SST foundation (and solar warming episodes are quite difficult to quantify) as frequently as would be requested to map the warming episode amplitudes. Daily amplitudes can be relatively easily mapped and localized amplitudes as large as 4 to 5 K are observed up to 80 North. It's difficult to simulate the large observed amplitudes unless we make extreme (unrealistic?) assumption on the preexisting density stratification. Further work at CMS will be devoted to better understand the origin of such large amplitudes and contribute to the Lake Vänern studies.

### References

Ciani, D., 2012, Diurnal variability of Sea Surface Temperature in the Mediterranean Sea: statistical description and model study, Master's thesis, Univ. La Sapienza, Roma

Eastwood, S., P. Le Borgne, S. Péré and D. Poulter, 2011, Diurnal variability in Sea Surface temperature in the Arctic, *Remote Sensing of Environment*, Volume 115, Issue 10, Pages 2594-2602

Péré, S, A. Marsouin and P. Le Borgne, 2013, Diurnal warming MDB: Examples and preliminary validation results, EUMETSAT 2013 conference proceedings, Vienna Austria, 16-20 Sept. 2013.

### 3.4 *GOTM in the Arctic* (Ioanna Karagali, DTU)

#### **Introduction**

Some of the ESA funded project SSTDV:REX-IMAM aims are to i) quantify and characterise the regional diurnal signals in the SEVIRI disk and ii) apply a 1-dimensional ocean turbulence model to describe the vertical temperature structure and thus bridge the gap between satellite and in situ estimates. The latter is achieved through the implementation of the General Ocean Turbulence Model (GOTM), which uses meteorological inputs either from in situ measurements or from NWP models, along with initial temperature and salinity profiles

Three different experiments are described below. A diurnal warming event identified in [1] during the 21st of June 2008 is modelled using NWP fields from HIRLAM and S, T profiles provided by the Norwegian Meteorological Institute (MetNo). Using the diurnal warming match-up database described in [2], buoys WMO 62926 & 44942 are selected for the period 14-22 July 2012.

#### **Data**

Modelled outputs for the wind speed, surface pressure, dry air temperature, cloud cover and humidity are obtained from ECMWF, for the WMO drifter experiments, and the Norwegian Meteorological Institute's (MetNo) HIRLAM12 for the June 2008 event.

Initial temperature and salinity profiles are obtained from the World Ocean Atlas 2009 dataset [3; 4] and the UK Met Office's EN3 dataset [5]. Temperature and salinity profiles for the June 2008 event are also provided by MetNo.

#### **Model Set-Up**

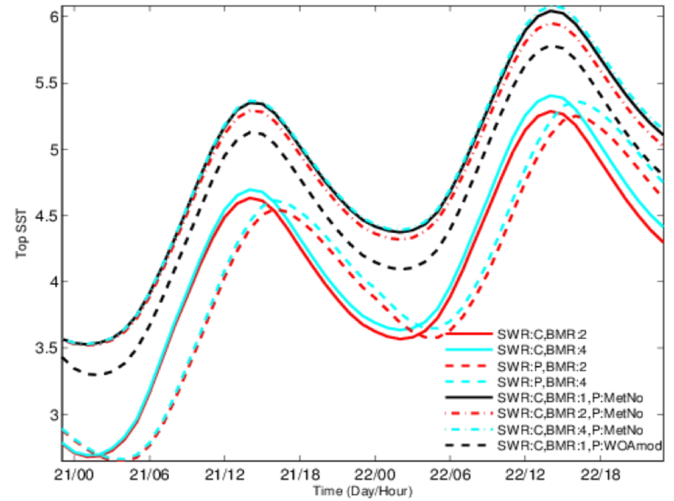
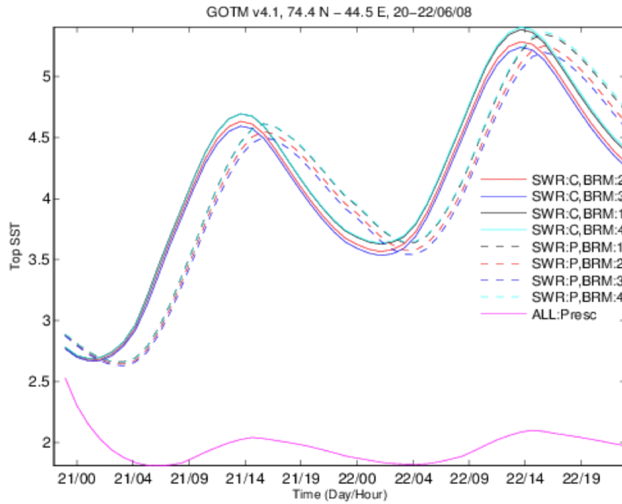
The GOTM v4.1 is used, consisting of 3 main packages. Surface heat and momentum fluxes are controlled by the 'airsea' package, which allows separation of the incoming shortwave radiation from the net heat flux. Fluxes can be directly prescribed (from an NWP model) or calculated from input meteorological fields (also typically obtained from NWP models).

The 'turbulence' package allows for the selection of the turbulence scheme used by the model. For the experiments presented here, the turbulence model calculates the kinetic energy (TKE) using a dynamic equation of  $k_\epsilon$  style while the dissipative length scale is computed using either a dynamic dissipation rate (LS:08) or a generic length scale (LS:10).

The 'obs' package allows to set different input parameters, such as the temperature and salinity profiles and the light extinction (LE) scheme amongst others. For the latter, a 2-band parametrisation is used that requires a set of three coefficients, representing different water types according to the Jerlov classification.

#### **Results**

The diurnal warming event described in [1] occurred around 74.4 N, 44.5 E at a depth of 250-300 m, had a skin SST of 3 °C when the event started and a maximum SST of 6 °C. As the WOA09 profile was too cold compared to the satellite SST, the upper profile layer was initially set to 3 °C. Figure 11a shows a 2-day run using different methodologies to calculate the surface fluxes. The most striking feature is that GOTM is able to reproduce a cycle that almost reaches up to 5.5 °C, when all surface fluxes are calculated from the meteorological parameters. There is a difference in the cycle when the shortwave radiation is directly prescribed from the MetNo HIRLAM12 files, both in amplitude and timing (solid versus dashed lines). When all fluxes are prescribed from HIRLAM12 (magenta solid line), the diurnal cycle is almost non-existent.



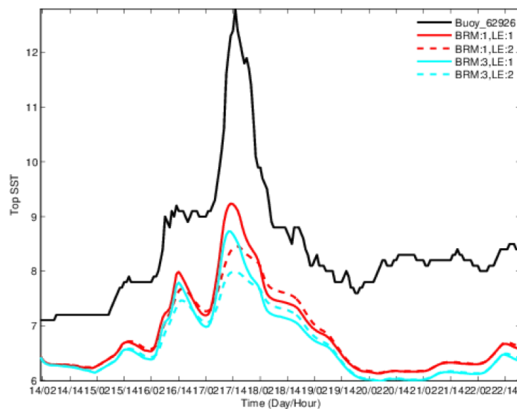
a)

b)

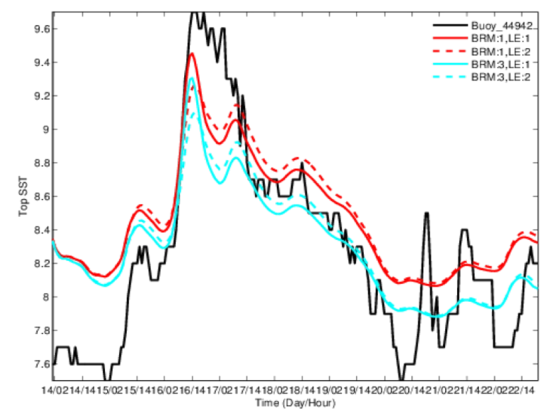
Figure 11: GOTM runs for different set-ups using calculated (C) or prescribed (P) surface fluxes and short-wave radiation (SWR), different methods for the calculation of the outgoing fluxes (BRM) and different profiles (WOA vs MetNo)

When the initial temperature and salinity profiles are obtained from MetNo, Figure 11b indicates that the starting temperature is higher and the whole diurnal amplitude is shifted, reaching to 6 °C. To investigate if the entire profile or only the upper layer of it modifies the temperature evolution, the WOA profile's top layer was modified to fit the MetNo profile's top layer. The dashed black lines indicates that while the top layer temperature does shift the whole temperature curve significantly, it is the entire profile that matters.

When different light extinction schemes are used, with LE:1 corresponding to Jerlov-I type and LE:4 to Jerlov-IB type, Figure 1 indicates that higher diurnal amplitudes are achieved by GOTM when using the most clear water type. This is opposite to what one would expect, as typically particles in the water reduce the light penetration depth, thus trapping it in the upper water layer where it is available for warming.



a)



b)

Figure 12: GOTM runs versus drifting buoy measurements (black solid) for two WMO buoys, a) 62926 and b) 44942.

The GOTM runs for the two drifting buoys are shown in Figure 3, for different set-ups testing the light extinction scheme and the method for outgoing heat. For Buoy 62926, Figure 3a

shows that while GOTM can resolve the diurnal variability, the amplitude of the signal is smaller than what is measured by the drifter. The event on the 17th of July exceeds 3 degrees and reaches temperatures of more than 12 °C but GOTM shows a maximum amplitude of 2 degrees and a peak temperature of 9 °C. For Buoy 44942, in Figure 3b, the measurement signal is rather noisy but GOTM even though starting warmer generally reproduces the diurnal variations and almost reaches the peak amplitude of the event on the 16th of July. Regarding the different GOTM set-ups, the BMR method 1, according to Clark et al. (1974) [6], gives higher amplitudes of diurnal warming in both drifting buoy cases.

### Summary and Conclusions

In summary, it has been shown that the 1-dimensional ocean turbulence model GOTM shows a promising ability in reproducing the diurnal variations observed from satellite and in situ sensors. When meso-scale NWP (HIRLAM12) outputs are used for the GOTM initiation and local initial profiles, it is found that the reproducible signal approximates more the observed case, as was shown for the 21st June 2008 case from [1]. When coarser NWP fields are used along with climatological profiles (WOA09), the modelled signal shows the correct variability but does not reach the correct amplitude. In addition, as GOTM includes a variety of adjustable parameters, identification of those important for the reproducibility of the observed diurnal signals is required. In particular, allowing GOTM to calculate the surface fluxes from input meteorological parameters has been found to allow for better reproducibility of the observed signals and the light extinction method also modifies the amplitude of the modelled signal. Currently a 9-band parameterisation is tested in GOTM following the implementation in [7].

### References

- [1] Eastwood, S. , P. Le Borgne , S. Péré and D. Poulter, 2011, *Diurnal variability in Sea Surface temperature in the Arctic, Remote Sensing of Environment, Volume 115, Issue 10, Pages 2594-2602*
- [2] Péré, S, A. Marsouin and P. Le Borgne, 2013, *Diurnal warming MDB : Examples and preliminary validation results, EUMETSAT 2013 conference proceedings, Vienna Austria, 16-20 Sept. 2013.*
- [3] Locarnini, R. A., A. V. Mishonov, J. I. Antonov, T. P. Boyer, H. E. Garcia, O. K. Baranova, M. M. Zweng, and D. R. Johnson, 2010. *World Ocean Atlas 2009, Volume 1: Temperature.* S. Levitus, Ed. NOAA Atlas NESDIS 68, U.S. Government Printing Office, Washington, D.C., 184 pp.
- [4] Antonov, J. I., D. Seidov, T. P. Boyer, R. A. Locarnini, A. V. Mishonov, H. E. Garcia, O. K. Baranova, M. M. Zweng, and D. R. Johnson, 2010. *World Ocean Atlas 2009, Volume 2: Salinity.* S. Levitus, Ed. NOAA Atlas NESDIS 69, U.S. Government Printing Office, Washington, D.C., 184 pp.
- [5] Ingleby, B., and M. Huddleston, 2007: *Quality control of ocean temperature and salinity profiles - historical and real-time data.* *Journal of Marine Systems*, 65, 158-175  
10.1016/j.jmarsys.2005.11.019
- [6] Clark, N. E., L. Eber, R. M. Laurs, J. A. Renner, and J. F. T. Saur, *Heat exchange between ocean and atmosphere in the Eastern North Pacific for 1961-1971, Tech. Rep. NMFS SSRF- 682, NOAA, U.S. Dept. of Commerce, Washington, D.C., 1974.*
- [7] Hallsworth S, *Modelling the diurnal variation of sea surface temperature using a one-dimensional ocean turbulence model.* PhD Thesis, University of Edinburgh, 2005.

### 3.5 Vertical profiles in the Arctic (Cristina Luis, met Norway)

#### Summary

There is much interest in the data available from gliders, buoys, and ships in the form of vertical temperature and/or salinity profiles, especially in their potential to be used in investigations of diurnal warming in the arctic. Vertical profile data is available from the Institute of Marine Research (imr.no), and downloadable via MyOcean, and this is a short summary of preliminary investigation of the data.

Most of the profiles available do not include data to the surface, instead reaching a minimum depth of 2-8m. A small number of ship and profiler/glider data sets (< 10% of total) have data recorded up to 0m/0db depth, an example of which is shown in Error: Reference source not found. Unfortunately, floats which collect data all the way to the surface (generally «unpumped» ARGO floats) do not have single identifying attribute, requiring inspection of the data to see if it is suitable.

In contrast to gliders, whose positions are variable throughout the year, there are several research vessels which cover the same transects year after year, often several times in the same year, which means data is available for repeat locations. Examples of transect routes with corresponding vessel names is available from IMR.

### Future

Acquire or develop and share a listing of WMO platform codes for profilers that record data to the surface.

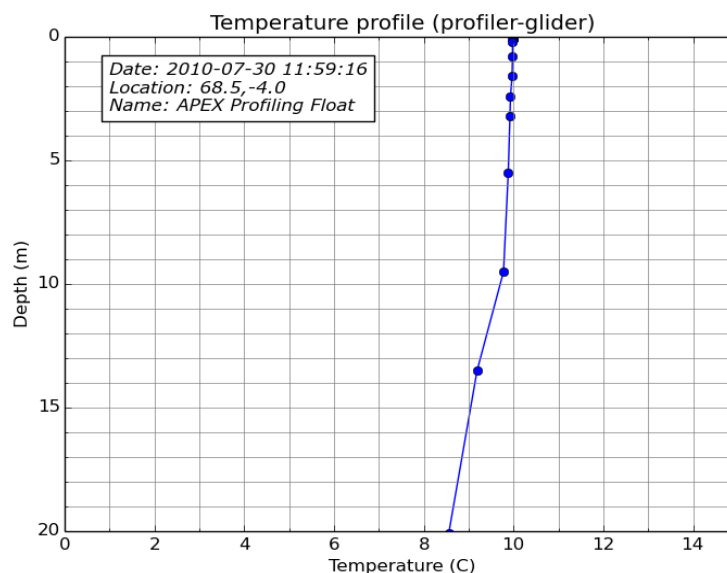


Figure 13: Argo float temperature profile example

#### 4. Summary report of session 4 : Solutions (J. Høyer, DMI)

The previous sections 1-3 focused upon the latest developments and challenges within SST retrievals and analysis in the Arctic. This section describes the best way forward to solve these issues. There was consensus within the group, that increased cooperation is the way forward, and that we should try to facilitate collaboration, both within the group and with external projects.

##### **Cooperation within the group:**

A list of tasks and projects between two or more institutions that could help facing the challenges, were identified within the group. The projects are listed below and the responsible persons are stated in the parenthesis. Where no names are given, the responsibility lies on all the participants at the workshop:

- Publish the workshop results, either as a report or in the journal: *Geoscientific Instrumentation, Method and Data Systems*. (Jacob and Pierre)
- Small projects, 2-4 partners,
  - Atmospheric profile data set (Jacob, Herve, Steinar, Cristina)
  - SST and ice concentration relationships (Jacob, Emma)
  - Wiki set up (Steinar)
  - Include information + reader code on in situ obs in Wiki (All)
  - GOTM preliminary studies (Ioanna, Pierre, Sonia, Chris, Herve)
  - Skin effects in Arctic, using FOAM (Alison, Chris)
- Student projects involving several institutions (Chris)
- Visiting scientists within Earthtemp and OSI-SAF
- Larger projects: (Part of Horizon 2020)
- Focused meetings can be envisaged for the smaller projects, within the Earthtemp visiting scientists or OSI-SAF VS

##### **Cooperation with external project**

Several large national and international research projects exist today, with emphasis on the Arctic ocean conditions and dynamics. It is the understanding of the group that these projects rely on standard satellite SST products to assess e.g. climate change or decadal predictability. These projects are not aware of the special arctic conditions for the SST retrieval and analysis and would obviously benefit from increased cooperation with the Earthtemp group. In addition, we could benefit from working with the in situ and modeling community to solve some of the identified issues.

To facilitate collaboration with the international projects, a list of current projects, relevant to the Arctic satellite SST community, were gathered and contact persons were identified within the group. These projects and contact persons are listed below:

**NACLIM (Jacob)** (EU FP7, 2012-2017, 18 partners): Assess the quality and skill of climate predictions

**ICE-ARC (Jacob)**(EU FP7, 2014-2018): Focus is on the rapid retreat and collapse of the Arctic sea ice cover and to assess the climatic (ice, ocean, atmosphere and ecosystem) changes

**IAOOS (Pierre)**: Monitoring Arctic climate change, up to 40 platforms, Ocean and Ice, see figure 1 for a picture of the platform.

**Arctic ROOS (Jacob)**: Operational monitoring and forecasting of ocean circulation, water masses, ocean surface conditions, sea ice and biological/chemical constituents

**HadISST (Nick Rayner ?)**: Monthly fields of SST and sea ice concentration from 1870 to date

**ACCESS (Pierre):** Monitoring and modeling Arctic climate change in ocean, atm and sea ice  
**OSI SAF (Pierre+Herve):** algorithm development, operational processing AVHRR and VIIRS

**OSI SAF (Herve) S3-FA:** federated activity on High Latitude validation of SLSTR SST

**NAACOS (Jacob):** Ice obs + ocean modelling, setting out Ice mass balance buoys set out

**NORMAP (Steinar):** reprocessing of AVHRR GAC for SST And IST

**SST CCI 2 (Chris):** SST retrievals, cloud/ice masking

**MyOcean2 Arctic SST(Cristina) + IST level 4analysis(Jacob) + Diurnal analysis (Alison)**

**MERCATOR Blanc (Herve):** High resolution model re analysis from 2007 till 2014 over the Arctic

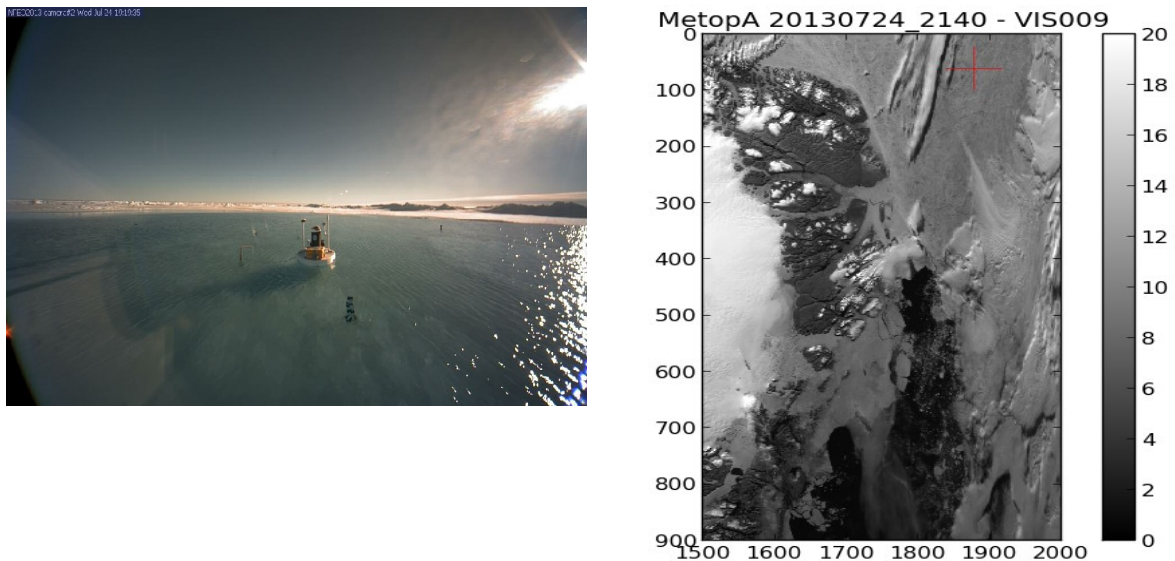


*Figure 1: N-E Greenland on the 24th of July 2013 at 21:40 UTC: left: A IAOOS buoy in a melt pond ; right: the same scene in the METOP-A/AVHRR channel 0.9 micron imagery. The dark spots around the buoy location (red cross) represent melt ponds.*

Through the discussions during the sessions and the collaboration projects, the meeting has resulted in increased collaboration within the group. This is obvious, already now, as several of the projects have already been kicked off and made progress one month after the meeting. A first Arctic atmospheric profile and simulation dataset has been built up and shared among partners; preliminary contacts have been set up with the IAOOS project: <http://www.iaos-equipex.upmc.fr/fr/index.html> (See Fig.1 showing the same melt ponds seen by an IAOOS buoy and METOP-A NE of Greenland)

We can thus conclude that such a focused meeting has been a success.